JOURNAL OF MATERIALS SCIENCE 29 (1994) 2801–2805

Formation of calcium chromate hydroxylapatite on the surface of a calcium-doped lanthanum chromite sintered body

I. YASUDA*, T. HIKITA
Fundamental Technology Research Laboratory, Tokyo Gas Co., Ltd, Shibaura, Minato-ku, Tokyo, 105 Japan

Sintered bodies of highly sinterable calcium-doped lanthanum chromites with chromium deficiency have been found to deteriorate and form calcium chromate hydroxyl apatite on their surfaces when exposed to high-temperature water-containing atmospheres. Microstructure analysis, composition measurement, and phase identification were performed on the surface of the samples after annealing in various conditions. The mechanism of the surface deterioration is thus deduced: traces of liquid phase which are formed in the sintering process migrate to the external surface and then react with water vapour to yield an apatite-type compound. Electrical conductivity has also been measured. The poorly conductive nature of the surface will cause some problems when the subject materials are used as high-temperature electronic conductors.

1. Introduction

Acceptor-doped lanthanum chromites have been attracting much attention because of their high electrical conductivity and chemical stability both in reducing and oxidizing atmospheres at high temperatures. Because of these excellent properties, these materials are widely accepted as candidates for interconnectors or separators of solid oxide fuel cells (SOFC). Recently, Sakai *et al.* [1] reported that calcium-doped lanthanum chromites (LCC) with chromium deficiency or calcium excess could be sintered to nearly full density at moderate temperatures in air. They also proposed that sintering proceeds via a liquid-phase sintering mechanism [2]. As yet, however, no long-term chemical stability of LCC in a practical fuel cell operating condition has been verified. In order to check the applicability of LCC, we have fabricated and tested short cell stacks with a planar configuration incorporating bipolar separator plates made of sintered LCC [3]. In a post-test analysis, a slight discolouration and change in surface morphology were observed. This paper describes the surface deterioration of sintered LCC in high-temperature water-containing atmospheres.

2. Experimental procedure

2.1. Sample preparation

Powders of reagent grade La_2O_3, $CaCO_3$ and Cr_2O_3 (Soekawa Chemicals) were mixed with a sufficient amount of ethanol and were ball-milled for 24 h. The resulting homogeneous powder mixture was dried and calcined at 1000–1200 °C in air for 12 h. This calcination procedure was repeated until the reaction product was confirmed by the powder X-ray diffraction analysis to be of a single-phase perovskite structure.

The raw materials thus obtained were uniaxially pressed into pellets of 22 mm diameter and 2–3 mm thick, and sintered at 1450–1600 °C in air for 3 h. The density of the sintered body exceeded 95% of the theoretical value with the exception of sample 305, whose excessive calcium content was very small. The sintered samples were then mirror-polished so that any change in surface morphology could be easily recognized after exposure to various atmospheres. Some portions of the starting powder mixture and the pulverized sintered body were fused with sodium peroxide and then dissolved in nitric acid. Their compositions were analysed by the ICP spectroscopy. It was confirmed that the metallic ratio of the starting powder mixture remained unchanged after sintering. Table I shows the nominal compositions of the samples thus determined.

2.2. Annealing

The sample pellets were wrapped with a platinum net and suspended by a PtRh 13 thermocouple in a quartz reactor tube that was placed in the centre of an electric furnace. Air and 4% H_2–N_2 gas, humidified at 69 °C, were passed through the reactor tube to control the surrounding atmosphere. The corresponding compositions of the oxidizing and reducing gases were

*Author to whom all correspondence should be addressed.

0022–2461

TABLE I Nominal sample composition determined by the ICP spectroscopy

Metallic element	Sample number						
	350	330	320	310	305	220	210
La	0.70	0.70	0.70	0.70	0.70	0.80	0.80
Ca	0.35	0.33	0.32	0.31	0.305	0.22	0.21
Cr	1.00	1.00	1.00	1.00	1.00	1.00	1.00

air/H_2O = 70/30 and $N_2/H_2/H_2O$ = 67.2/2.8/30, respectively. The reason for the humidification is that the presence of water vapour seemed to accelerate the surface deterioration. The annealing temperatures were 500, 700, 850 and 1000 °C. The samples were heated to the annealing temperature, kept for a desired holding time, and then furnace-cooled to room temperature. The holding time was 12, 24, 48 and 120 h.

2.3. Analysis

The microstructure of the surface after annealing was examined by an optical microscope (OM) and a scanning electron microscope (SEM; JEOL JSM-5400). The metallic composition of the surface was determined by the energy-dispersive X-ray analyser (EDX; JEOL JED-2001). The surface phase was identified by the small-angle X-ray diffractometry using CoK_α radiation with an injection angle of 0.3° (Phillips PW 1710).

The electrical conductivity of the surface layer was measured by the standard four-probe method at ambient temperature. The inter-distance between the needles was 1 mm. Because the resistivity of the surface layer seemed fairly high, the current was controlled so that the voltage difference between the voltage probes did not exceed 10 mV.

3. Results

3.1. Change in surface morphology

Fig. 1 shows optical microscopic views of the surface of sample 350 before and after annealing. Fig. 1a–c show the surface of as mirror-polished, after annealing in air/H_2O at 1000 °C for 48 h, and after annealing in $N_2/H_2/H_2O$ at 1000 °C for 48 h, respectively. The dark irregular spots with a size of a few to 20 μm are residual macropores that could not be removed in the green formation process. Comparing the surface morphology of (b) and (c) with that of (a), remarkable changes can be observed, suggesting that some kind of surface deterioration occurred during the annealing. In the case of annealing in the oxidizing atmosphere, the original smooth surface (a) is completely lost and a newly emerged layer seems to have covered the entire area as shown in (b). However, in (c), we see some "islands" that have white grains in the centre surrounded by a belt of very fine blue–green particles (c). This occurred when the samples were annealed in the reducing atmospheres.

For more detailed inspection, SEM/EDX analysis was performed on the surface indicated in Fig. 1b. The

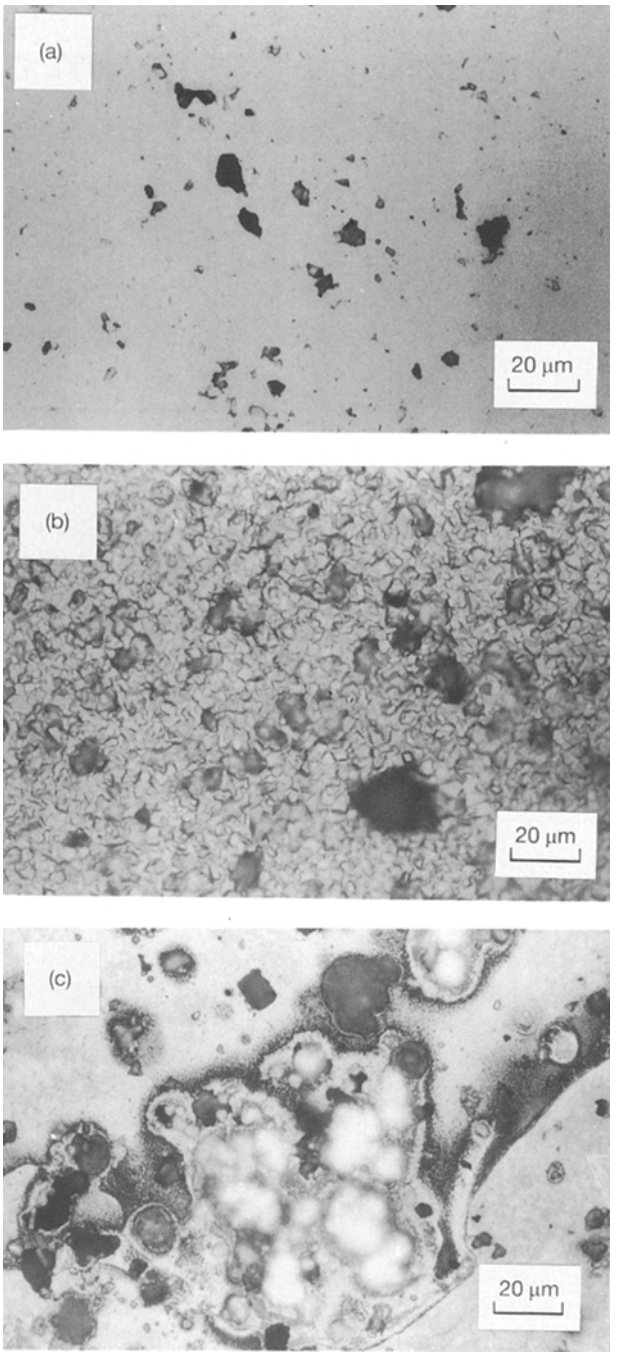

Figure 1 Optical microscopic views of the surface of sample 350: (a) as mirror-polished, (b) after annealing in air/H_2O at 1000 °C for 48 h, and (c) after annealing in $N_2/H_2/H_2O$ at 1000 °C for 48 h.

results are shown in Fig. 2. In the surface view (a), some faceted hexagons are found, indicating that crystalline phase with hexagonal symmetry appeared as a result of the surface deterioration. Fig. 2b presents an SEM image of the cross-section and Fig. 2c is the corresponding calcium distribution map. We can observe a dense surface layer about 4 μm thick with a columnar structure. It is also clearly envisaged that this layer is rich in calcium. Between the newly developed surface layer and the angular bulk grains are seen some devastated grains with an ambiguous shape.

3.2. Identification of deterioration products

In order to clarify the change in surface phase, small-angle X-ray diffraction analysis was conducted on the

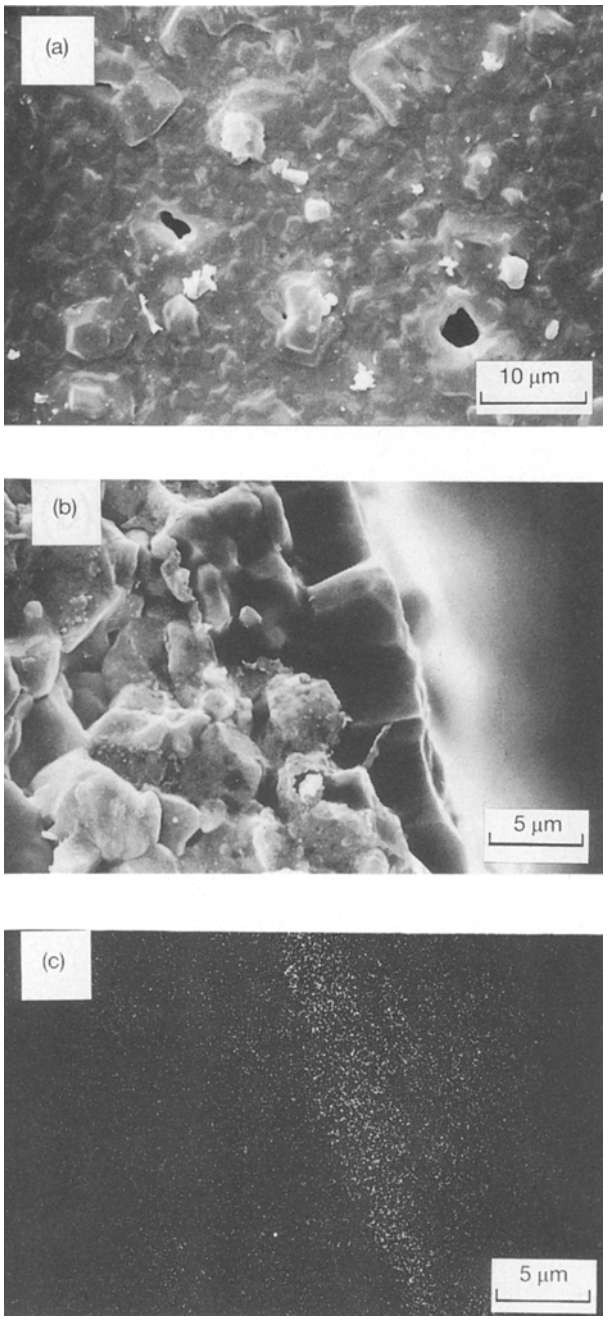

Figure 2 Scanning electron micrographs and calcium distribution map of sample 350 after annealing in air/H_2O at 1000 °C for 48 h: (a) surface view, (b) cross-sectional view, and (c) calcium distribution map.

surface shown in Fig. 1a and b. Fig. 3 shows the diffraction patterns together with the reference patterns in the JCPDS (Joint Committee in Powder Diffraction Standards) library. The surface of the sample before annealing is proved to possess a perovskite-type structure with orthorhombic symmetry (a). The post-annealing sample, however, gives a completely different diffraction pattern (b), which is identified as attributable to calcium chromate hydroxyl apatite, $Ca_5(CrO_4)_3OH$.

3.3. Effect of annealing conditions

Listed in Table II are the compositions of the surface and of the cross-section determined by the EDX analysis, and the identified surface phases for sample 350 that was treated under various annealing conditions. The composition of the cross-section is constant and gives the same value as that obtained for the as-sintered sample within experimental uncertainty. This result suggests that the deterioration proceeds only on the surface and that gaseous species (water vapour) in the atmosphere is involved in the reaction. From the results of the annealing experiments in the oxidizing atmospheres, it is clearly seen that the amount of apatite-type compound increases with increase in annealing temperature and holding time. The higher calcium concentration and the higher diffraction peak intensity obtained for the surface after annealing in the oxidizing atmospheres indicate that the reaction kinetics is faster in the oxidizing atmosphere than in the reducing atmosphere.

3.4. Surface conductivity

Regarding the apatite-type compound, $Ca_5(CrO_4)_3OH$, only a few reports on crystal structure [4, 5] and phase relations [6, 7] can be found in the literature. The paucity regarding electrical properties has prompted us to conduct electrical conductivity measurements. The resistivities of the samples were determined by the equation

$$\rho = 2\pi SV/I \quad (1)$$

where ρ, S, V, and I denote resistivity, inter-distance of probes, voltage and current, respectively. The results

TABLE II Composition, phase present and surface conductivity of LCC sample 350 after annealing in water-containing atmospheres

Atmosphere	Temperature (°C)	Annealing time (h)	Surface composition, La/Ca/Cr	Fracture surface composition, La/Ca/Cr	Phase present[a]	Surface conductivity (at RT) (10^{-6} S cm^{-1})
Air/H_2O (70/30)	1000	12	22.7/31.8/45.5	35.3/13.1/51.6	AP	47
		24	20.7/39.7/39.6	35.4/15.5/49.1	AP	–
		24	5.2/56.3/38.5	34.8/16.9/48.3	AP	3.8
		120	3.0/64.8/32.2	34.9/15.8/49.4	AP	4.2
	850	12	34.9/16.3/48.8	34.8/15.2/50.0	AP	–
		24	30.9/21.5/47.6	34.9/14.1/51.0	AP + P	–
		48	23.5/42.7/33.8	35.7/14.5/49.8	C + P	–
	700	48	37.7/15.5/46.8	35.4/15.9/48.7	AP + P	–
$N_2/H_2/H_2O$ (67/3/30)	1000	48	34.7/17.7/47.6	35.2/16.8/48.0	AP + P	–
	850	48	35.8/15.3/48.9	36.1/14.3/49.6	P	–

[a] AP, apatite phase $Ca_5(CrO_4)_3OH$; P, perovskite phase; C, $CaCO_3$ phase.

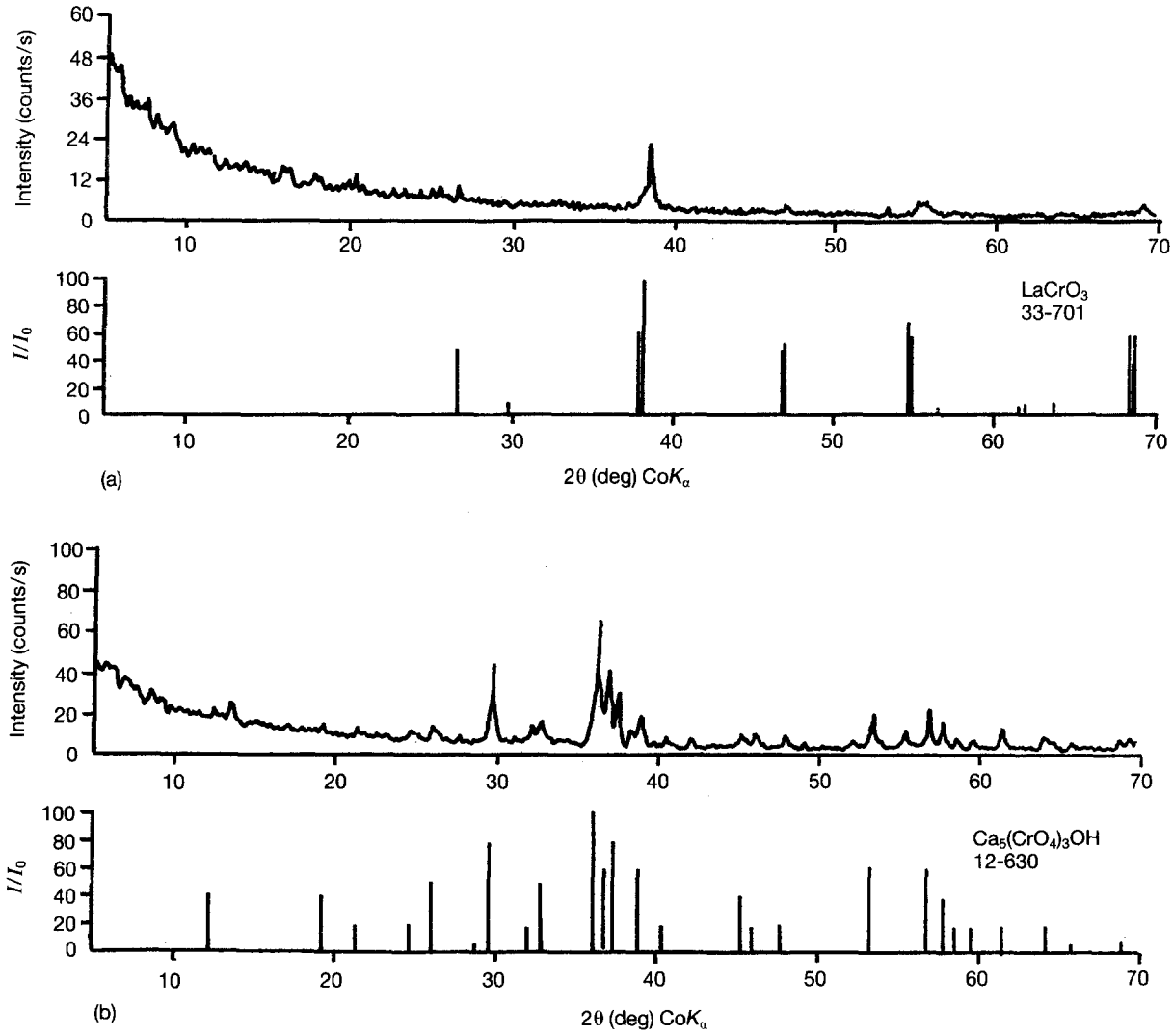

Figure 3 X-ray diffraction patterns of the surface of sample 350 (a) before and (b) after annealing in high-temperature water-containing atmospheres.

are also shown in Table II. The surface conductivity of the samples after the annealing is in the order of 10^{-6} and 10^{-5} S cm^{-1}, which is five or six orders of magnitude lower than that of the original LCC. Such high resistivity in the surface layer will cause significant problems when it comes to applications as electronic conductors.

For the cases where no results are given, conductivities attributable to doped lanthanum chromites were observed. The reason for this may be that the surface layer was so thin that the probes penetrated it, or that the surface coverage of the apatite-type compound was so sparce that the tip of the probe contacted an intact part.

3.5. Effect of composition

Fig. 4 shows optical microscopic views of the surface of samples 310 and 210 after annealing in the oxidizing atmospheres at 1000 °C for 48 h. As can be seen both in (a) and (b), most of the surface has preserved its original smoothness although many bar-shaped grains are found. This kind of microstructure is considered to be that of an initial stage of nuclei formation and grain growth. From the fact that the grains of the deterioration product in sample 310 have larger size and more well-defined shape than those in sample 210, it is deduced that the kinetics of the surface deterioration is faster for the compositions with heavier calcium doping and more calcium excess (i.e. chromium deficiency).

4. Discussion

From the experimental results given above, we can assume the following deterioration mechanism. The LCC with chromium deficiency is supposed to be densified through a liquid-phase sintering mechanism [2]. In general, it is desirable that the intermediate compounds formed in the sintering process diminish in the final stage of sintering. In the present system, however, traces of liquid phase seem to remain in or near the grain boundaries, rapidly diffuse towards the external surface, and then react with water vapour to yield an apatite-type compound.

The proposed mechanism offers a possibility for eluding practical problems by squeezing the traces of liquid phase during a sufficiently long-term annealing and by removing the resulting deteriorated layer before use. However, samples thus treated continued to

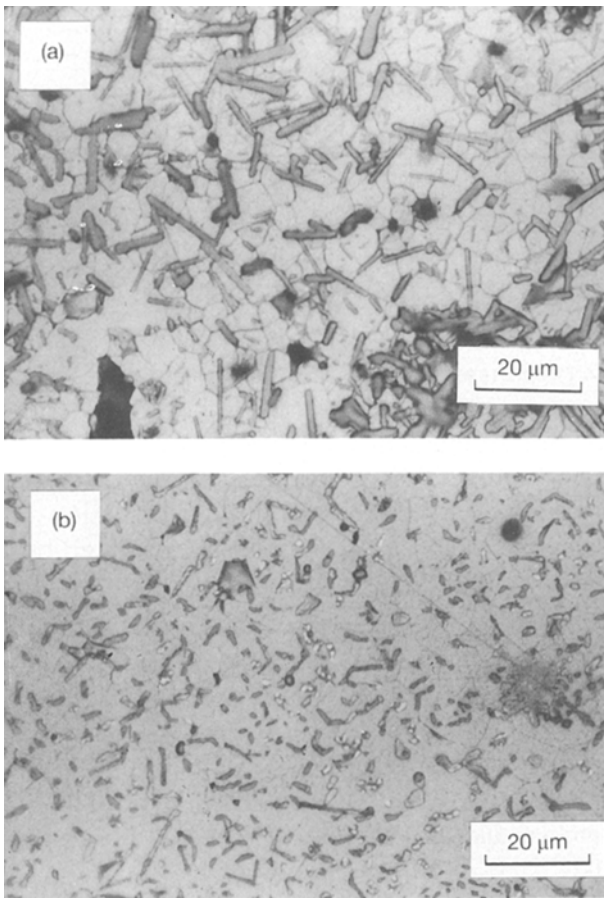

Figure 4 Optical microscopic views of the surface after annealing in air/H_2O at 1000 °C for 48 h: (a) sample 310 and (b) sample 210.

show the surface deterioration after reannealing. Repeating the squeezing–polishing–reannealing process always gave the same results, contrary to our expectations. Once the apatite-type compound entirely covers the surface, its extreme density hinders direct contact of the sources and water vapour as shown in Fig. 2b, which leads to apparent cessation of the deterioration.

Based upon these considerations, we have come to the conclusion that it is necessary to reduce the amount of intermediate compounds within the limits of high sinterability. The effective methods for this will be (1) to reduce calcium doping, (2) to reduce calcium excess or chromium deficiency, (3) to calcine and sinter at higher temperatures, and (4) to employ a sophisticated powder synthesis process whereby composition fluctuation can be eliminated. The effectiveness of (1) and (2) have, in reality, been shown in the preceding subsection. The significance of (4) has recently been reported by Sakai *et al.* [8].

5. Conclusion

Sintered bodies of highly sinterable calcium-doped lanthanum chromites with calcium excess or chromium deficiency have been found to deteriorate and form calcium chromate hydroxyl apatite on the surface in high-temperature water-containing atmospheres. The surface deterioration proceeds via a rapid diffusion of liquid-phase traces towards the external surface followed by reaction with water vapour in the surrounding atmosphere. The rate of deterioration increases with increase in doping level and calcium excess (i.e. chromium deficiency). Reducing these two variables is therefore effective for preventing the deterioration. In order to identify specifically the problems caused by the surface deterioration, further investigation will be required on the apatite-type compound, $Ca_5(CrO_4)_3OH$. Knowledge remains lacking regarding phase relations, electrical properties, and chemical compatibility with other SOFC components.

References

1. N. SAKAI, T. KAWADA, H. YOKOKAWA, M. DOKIYA and T. IWATA, *J. Mater. Sci.* **25** (1990) 4531.
2. N. SAKAI, T. KAWADA, H. YOKOKAWA and M. DOKIYA, in "Proceedings of the 2nd International Symposium on Solid Oxide Fuel Cells", Athens, July 1991, edited by F. Grosz, P. Zegers, S. C. Singhal, and O. Yamamoto (Commission of the European Communities, Luxembourg, 1991) p. 629.
3. I. YASUDA, T. KAWASHIMA, T. KOYAMA, Y. MATSUZAKI and T. HIKITA, in "Proceedings of the International Fuel Cell Conference," Makuhari, February 1992 (New Energy and Industrial Technology Development Organization, Tokyo Japan) p. 357.
4. V. R. SCHOLDER and H. SCHWARZ, *Z. Anorg. Allgem. Chem.* **326** (1963) 11.
5. M. A. JOHNSON, *Mineral Mag.* **32** (1960) 408.
6. Z. PANEK and E. KANCLIR, *Silikaty* **20**(2) (1976) 113.
7. M. HAVIAR, V. FIGUSCH and G. PLESCH, *Sci. Sintering* **12**(2) (1980) 119.
8. N. SAKAI, T. KAWADA, H. YOKOKAWA and M. DOKIYA, in "Extended Abstracts of the 17th Symposium on Solid State Ionics, Japan", Japan, Nagoya, November 1991, p. 89.

Received 15 June 1992
and accepted 9 August 1993